

Difference in dynamic properties of photoreceptors in a butterfly, *Papilio xuthus*: possible segregation of motion and color processing

Masashi Kawasaki^{1,2} · Michiyo Kinoshita¹ · Matti Weckström³ · Kentaro Arikawa¹

Received: 13 July 2015 / Revised: 16 August 2015 / Accepted: 17 August 2015 / Published online: 2 September 2015
© Springer-Verlag Berlin Heidelberg 2015

Abstract The eyes of the Japanese yellow swallowtail butterfly, *Papilio xuthus*, contain six spectral classes of photoreceptors, each sensitive either in the ultraviolet, violet, blue, green, red or broadband wavelength regions. The green-sensitive receptors can be divided into two subtypes, distal and proximal. Previous behavioral and anatomical studies have indicated that the distal subtype appears to be involved in motion vision, while the proximal subtype is important for color vision. Here, we studied the dynamic properties of *Papilio* photoreceptors using light stimulation with randomly modulated intensity and light pulses. Frequency response (gain) of all photoreceptor classes shared a general profile—a broad peak around 10 Hz with a declining slope towards higher frequency range. At 100 Hz, the mean relative gain of the distal green receptors was significantly larger than any other receptor classes, indicating that they are the fastest. Photoreceptor activities under dim light were higher in the ultraviolet and violet receptors, suggesting higher transduction sensitivities. Responses to pulse stimuli also distinguished the green receptors from others by their shorter response latencies. We thus concluded that the distal green receptors carry high frequency information in the visual system of *Papilio xuthus*.

Keywords Butterfly vision · Motion vision · Color vision · Photoreceptor dynamics

Abbreviations

B	blue
BB	broadband
G	green
dist-G	distal green
prox-G	proximal green
LED	light-emitting diode
R	red
UV	ultraviolet
V	violet

Introduction

Stationary and dynamic properties of sensory signals are often processed by separate parallel sensory subsystems, such as the parvocellular and magnocellular visual pathways of primates (Livingstone and Hubel 1988). Similar segregation appears to be present also in insects. In flies, different subsets of photoreceptor cells feed inputs to distinct pathways: a set of photoreceptors terminating in the first visual neuropil, the lamina, have identical broadband spectral sensitivity, while those projecting long axons directly into the second visual neuropil, the medulla, express variable narrow spectral sensitivities (Friedrich et al. 2011). This suggests that at least in flies the primary function of the lamina is to process achromatic information, while the medulla is the region where chromatic processing begins (Hardie 1985; Strausfeld and Lee 1991; Wardill et al. 2012; but also see Schnaitmann et al. 2013). Interestingly, the fly broadband photoreceptors with short axons terminating in the lamina respond to light stimuli

✉ Masashi Kawasaki
mk3u@virginia.edu

¹ Laboratory of Neuroethology, SOKENDAI (The Graduate University for Advanced Studies), Hayama, Japan

² Department of Biology, University of Virginia, Charlottesville, VA 22904, USA

³ Centre for Molecular Materials, Biophysics, University of Oulu, Oulu, Finland

much faster than the spectral receptors with long axons (Anderson and Laughlin 2000).

The photoreceptors with fast dynamics are likely to be involved in motion vision, where this property is much more of essence than, e.g., in color vision. In insects, motion information is processed in the lobula plate, a subdivision of the third visual neuropil. Motion-sensitive neurons in the lobula plate are often achromatic, which corresponds to the achromatic nature of motion-dependent behaviors such as optomotor response (Kaiser 1975; Yamaguchi et al. 2008), distance measurement during flight (Lehrer et al. 1989), and visual scanning (Lehrer et al. 1985). These behaviors of trichromatic bees (KV Frisch 1914; Dyer and Arikawa 2014) appear to be driven by photoreceptors whose spectral sensitivity peaks in the green wavelength region (G receptors). These cells in fact have faster dynamics than the ultraviolet (UV) and blue-sensitive (B) receptors (Skorupski and Chittka 2010; Vähäkainu et al. 2013).

The bee eyes consist of ommatidia with nine photoreceptors, R1–9. Each ommatidium contains seven G receptors and two short wavelength (i.e., UV and B) receptors in one of three possible combinations, UV–B, UV–UV, or B–B. This makes the eyes a collection of three spectrally heterogeneous ommatidia, which are randomly distributed in the hexagonal array (Wakakuwa et al. 2005). The G receptors are not merely having faster dynamics, compared to the short-wavelength receptors, but are also embedded in all ommatidia without making any gap in the hexagonal lattice of ommatidia: G receptor system therefore provides the highest possible spatial resolution, which must be beneficial for motion as well as shape vision.

The spectral organization of the eye is more complex in several groups of butterflies (Wakakuwa et al. 2007). The Japanese yellow swallowtail, *Papilio xuthus*, uses sophisticated color vision when searching for flowers (Kinoshita and Arikawa 2014), and their eyes are furnished with at least 6 classes of spectral receptors, which are of the ultraviolet (UV), violet (V), blue (B), green (G), red (R) and broadband (BB) classes. These receptors are embedded in the ommatidia in three fixed combinations (Arikawa 2003). Here again, all ommatidia contain at least two G receptors. A subset of the G receptors contributes to form the distal tier of the rhabdom and they are called distal green (dist-G) receptors. The dist-G receptors send axons to the lamina and terminate there. Unlike all other photoreceptors whose axons bear fine processes in the lamina and are mutually connected via synapse-like structures, the axons of dist-G receptors are thicker and smoother, and without any connections with other photoreceptors, suggesting that they could constitute an independent system that may be adequate for fast signaling (Takemura et al. 2005; Takemura and Arikawa 2006).

On the other hand, wavelength discrimination of foraging *Papilio xuthus* has indicated that their color vision is

tetrachromatic based on UV, B, G and R receptors (Koshitaka et al. 2008). We assume that another subset of G receptors, the proximal R5–8 green (prox-G) receptors that form the proximal tier of the rhabdom in one of the ommatidial types, contributes to the color vision system (Kinoshita et al. 2006). If the prox-G receptors were in fact involved in color vision, one would assume that the dynamics of the prox-G receptors might be slower than that of the dist-G receptors.

Here, we recorded voltage responses of photoreceptors to light with randomly modulated intensity, as well as to light pulses. We compared the dynamic properties between the photoreceptor classes, and found that the dist-G receptors indeed have faster dynamics than any other classes of spectral receptors.

Materials and methods

Animals

We used newly emerged adults of both sexes of the Japanese yellow swallowtail butterfly, *Papilio xuthus*. They were taken from a laboratory culture, which was derived from eggs laid by females captured in the field around Sokendai. The hatched larvae were fed on fresh citrus leaves at 25 °C under a light regime of 10 h light: 14 h dark, which induces pupal diapause. The diapausing pupae were kept at 4 °C for at least 3 months, and allowed to emerge at 25 °C. The emerged adults were fed daily with 5 % sucrose solution and used from 2 to 5 days after emergence.

Electrophysiology

A butterfly was mounted dorsal side up on a plastic stage with bees wax. A small opening (~300 μm) was made on the dorsal region of the eye, through which a glass capillary electrode filled with 1 M KCl was inserted vertically. The location of the opening was adjusted from preparation to preparation to acquire recordings from both the distal and proximal tiers of the ommatidia in the fronto-lateral looking region of the eye. Photoreceptor potentials in response to light flashes were recorded using an amplifier (Nihonkoden MEZ-8301) and an analog-to-digital converter (National Instruments PCI-6218, sampling frequency set at 2 kHz). The quality of intracellular recording was controlled by the following criteria: (1) resting potential was deeper than –40 mV, (2) drift of resting potential before and after the recording session was less than 10 mV, (3) magnitude of response to the brightest stimulus intensity was greater than 30 mV, (4) the spectral sensitivity class estimate was identical before and after the recording session, and (5) the

magnitude of hyperpolarizing responses to a light pulse did not exceed 5 mV.

Light stimulus and frequency responses

The light source consisted of packed LEDs of ultraviolet, violet, blue, green and red (UV, V, B, G, R in Fig. 1) whose emission peaks are, respectively, at 369, 396, 463,

523, and 612 nm (half-maximum widths of the emission spectra are 14, 14, 20, 33, and 16 nm, respectively), which match the spectral sensitivity maxima (360, 400, 460, 520, and 600 nm) of photoreceptors of *Papilio xuthus* (Arikawa et al. 1987). A selected type of LED was driven by a custom-made voltage-controlled constant-current circuit that in turn was driven by a digital-to-analog converter at the conversion frequency of 2 kHz. LED emission was

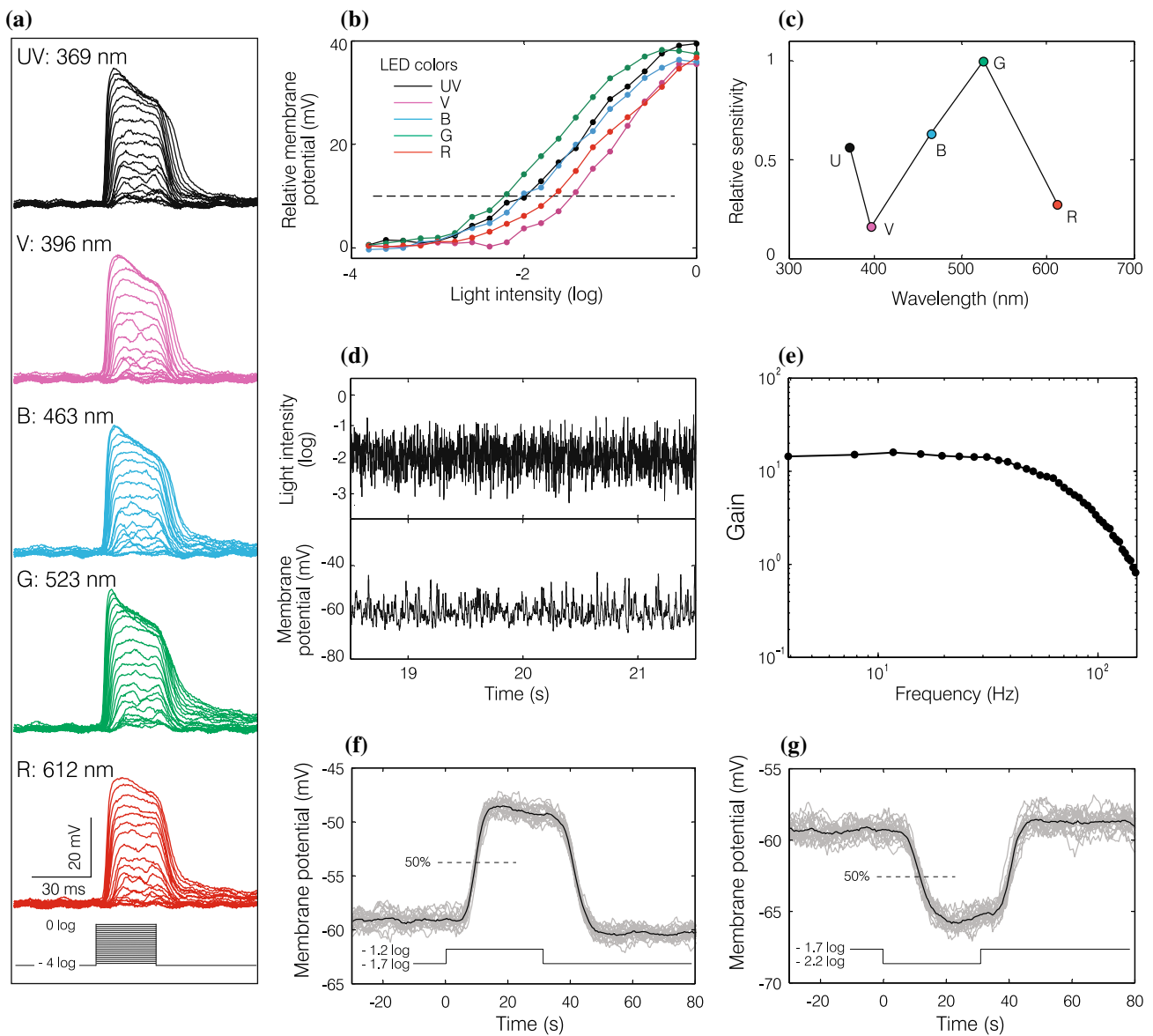


Fig. 1 A case of a representative photoreceptor (prox-G class) is given for illustration of recording and analysis methods. **a** 20 superimposed membrane potential responses (*top*) to incremental light pulses (*bottom*) from five types of LEDs. **b** Intensity–voltage curves derived from the responses in **a**. Y-axis indicates membrane potential relative to that before stimulation. **c** Inverse values of intensities necessary to evoke 10 mV of responses from the spectral sensitivity curve in **b** were normalized to the maximum showing spectral sen-

sitivity in relative term. **d** Time-series plot of a section of the light stimulus with random noise intensity modulation (*top*) and the corresponding membrane potential response (*bottom*). **e** The frequency response function between the stimulus and responses shown in **d**. **f** 20 traces of membrane potential responses to incremental pulses (*gray*) and their average (*black*). **g** 20 traces of membrane potential responses to decrement pulses (*gray*) and their average (*black*)

collected by a series of lenses and focused on a light guide (5 mm diameter) whose other end was mounted on a perimeter device 11 cm away from the eye surface, yielding a stimulus of 2.6° in size. The maximal light intensity, integrated over the wavelength range from 300 to 700 nm, was 7.6×10^{13} photons \cdot cm $^{-2}$ \cdot sec $^{-1}$ at the eye surface. The stimulus intensity ranged from $\log(I) = -4$ (minimum) to $\log(I) = 0$ (maximum).

Two temporal types of light stimuli, noise and pulse, were employed. The noise stimulus was a 60-s-long continuous light whose intensity was modulated at random. The random noise had a mean at the half-max intensity that evoked 50 % of maximum response of the 0 log stimulus when given as a 30-ms-long pulse in the dark-adapted case. The random modulation had a standard deviation of 0.5 log and bandwidth from DC to 200 Hz. The frequency response functions (the gain) were computed—via the cross-power spectra divided by input power spectra (Bendat and Piersol 1971; Juusola et al. 1994) with Welch's method, with 50 % overlap and 1024 point FFT window, between a noise stimulus and a membrane potential with a custom-made program package written in MATLAB (Mathworks, MA, USA). Cross-correlation functions were also computed between the noise stimulus and membrane potential as a measure of linearity. The pulse stimuli consisted of a train of 30-ms-long pulses ($n = 20$ at 500 ms interval) given either from dark or from the half-max level. For the latter case, light pulses were either incremental or decremental in intensity. Dynamic properties of responses were examined in the averaged responses ($n = 20$, Fig. 1). While the noise analysis describes photoreceptor's input–output properties as a linear system, the pulse analyses are capable of detecting non-linear components such as differences between increment and decrement responses. Spontaneous activities of photoreceptors ('dark noise') were recorded under a no-stimulus condition (< -5 log units) for 60 s. Power density spectra of the dark noise were also calculated with Welch's method as above.

Statistical testing

Statistical testing was done with OriginPro (Microcal, USA) using one-way ANOVA followed by multiple comparisons.

Recording sessions and classification of photoreceptors

After establishing intracellular penetration, the light guide emitting light pulses scanned over the visual field to find the optical axis of the receptor. All five types of LEDs simultaneously flashed during this search phase of the experiment. Then, a series of light pulses with increasing intensities (-4 log to 0 log with 0.2 log-unit steps) was

given every 500 ms to measure the intensity–voltage function (V-logI curve) using ultraviolet LEDs. The curve construction was then repeated using violet, blue, green and red LEDs. These procedures caused a moderately light-adapted state. Spectral sensitivity of the photoreceptor was computed as an inverse of interpolated stimulus intensity necessary to evoke 10 mV of depolarization for each LED type (Fig. 1a–c). The photoreceptors were then categorized into UV, V, B, G, R, and BB classes according to their spectral sensitivity. The UV, V, B, G, and R receptors showed their spectral peak to the peak emission wavelength of respective LED types. The BB receptors showed responses to blue, green and red LEDs that were all within 60 % of the maximum sensitivity (regardless of where the highest sensitivity was located), but less than 20 % sensitivity of the maximum to the UV stimulation (Arikawa et al. 2003). The G receptors were sub-divided into proximal green (prox-G) and distal green (dist-G) receptors (Kinoshita et al. 2006). The prox-G receptors were recognized when photoreceptor was more sensitive to red than to violet and blue LEDs (in contrast to dist-G receptors that show high short-wavelength sensitivity), and it was encountered in the same recording track where R or BB receptors were recorded. The rest of photoreceptors with the sensitivity peak at green wavelength were categorized into dist-G. Thus, we compared dynamic properties of seven photoreceptor classes, UV, V, B, prox-G, dist-G, R, and BB.¹

Results

Intracellular recording was made from 223 light-adapted photoreceptors, 72 of which met the inclusion criteria (see Methods). They are categorized into UV ($n = 8$), V ($n = 9$), B ($n = 13$), dist-G ($n = 13$), prox-G ($n = 7$), R ($n = 16$), and BB ($n = 6$).

Responses to noise stimuli

The photoreceptors were stimulated by light with randomly modulated intensity as shown in Fig. 1d. Analysis of the response with the stimulus yielded the photoreceptor gain (Fig. 1e). Mean gains from all photoreceptor classes commonly showed a broad peak around 10 Hz with a continuous decay towards higher frequencies with half maximum frequencies between 40 and 60 Hz (Fig. 2a). We compared

¹ Note that the abbreviation, dist-G, contains both 'double-peaked green (dG)' and 'single-peaked green (sG)' spectral classes in the distal tier in our previous publications (Arikawa et al. 1999). The B class in the current study contains both narrow-B and broad-B receptor subclasses described in Kinoshita et al. (2006).

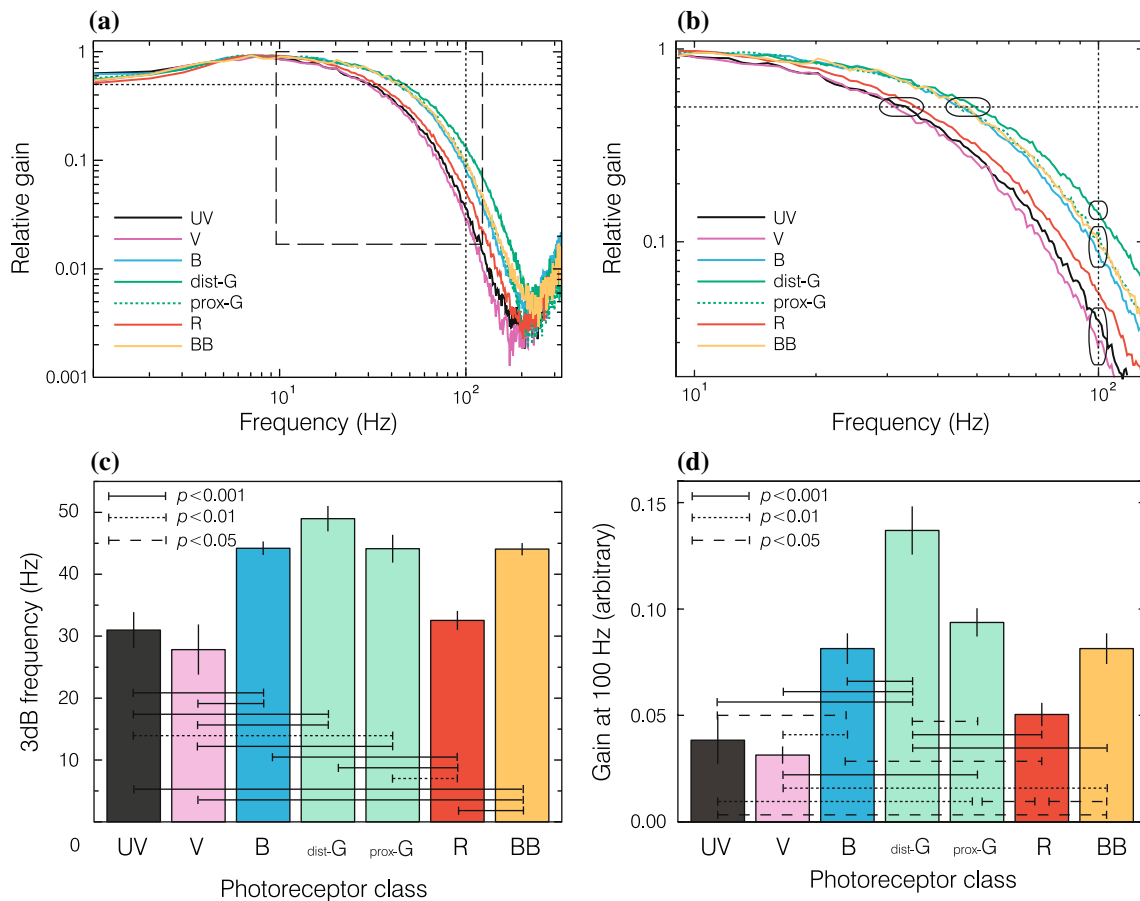


Fig. 2 Comparison of frequency spectra between photoreceptor types. **a** Mean spectra for different photoreceptor types normalized at the maximum. **b** Magnified view of the broken-squared area of **a**. *Ovals* indicate 3 dB frequency (*top two*) and gain at 100 Hz (*right three*). **c** Comparison of 3 dB frequency between photoreceptor types. **d** Comparison of gain at 100 Hz between photoreceptor types (one-way ANOVA follow by multiple comparisons)

the gain values at the 3 dB or corner frequency for each receptor class (horizontal dotted line in Fig. 2a) and at 100 Hz (vertical dotted line in Fig. 2a) between gain functions normalized at their maximum (6–10 Hz). Figure 2b shows an expanded version of the region in Fig. 2a as indicated by the broken-line square. At corner frequencies, gain values are different, the dist-G receptors having the greatest 3 dB values (Fig. 2c). At the frequency of 100 Hz, the difference becomes prominent: the gain value of dist-G receptors is significantly larger than that of any other receptor classes, followed by prox-G, B, and BB; the R, UV and V tended to be the slowest by that measure (Fig. 2d).

Responses to pulse stimuli

Spectral density functions presented above describe only the linear components of the system’s response. Convoluting the stimulus noise with the cross-correlation function resulted in less than 50 % of actual responses as estimated with root mean square, which means that significant

non-linear components are present in the photoreceptor responses. Incremental and decremental pulses from a steady level (Fig. 3a) and pulses from dark (Fig. 3b) were used to further explore response dynamics of the photoreceptors, because these stimuli efficiently evoke non-linearities (Marmarelis and Marmarelis 1978). The time required for the membrane potential to reach 50 % of the peak response was used as a measure of response latency. In response to incremental pulses given from half-maximum steady background, the dist-G and prox-G receptors showed shorter latency than the UV, V, and R receptors (Fig. 3c). For decrement pulses again, the latencies for the dist-G and prox-G receptors were shorter than those of the UV, V, and R receptors (Fig. 3d). When the pulses (+½ max) were given from dark, dist-G showed significantly shorter latencies than UV, V, and R, while prox-G’s latency was shorter than only UV (Fig. 3e). Response magnitudes of depolarization responses were consistently larger (~50 %) than those of hyperpolarizing responses in all photoreceptor classes (Fig. 3a). Also, latencies for depolarizing

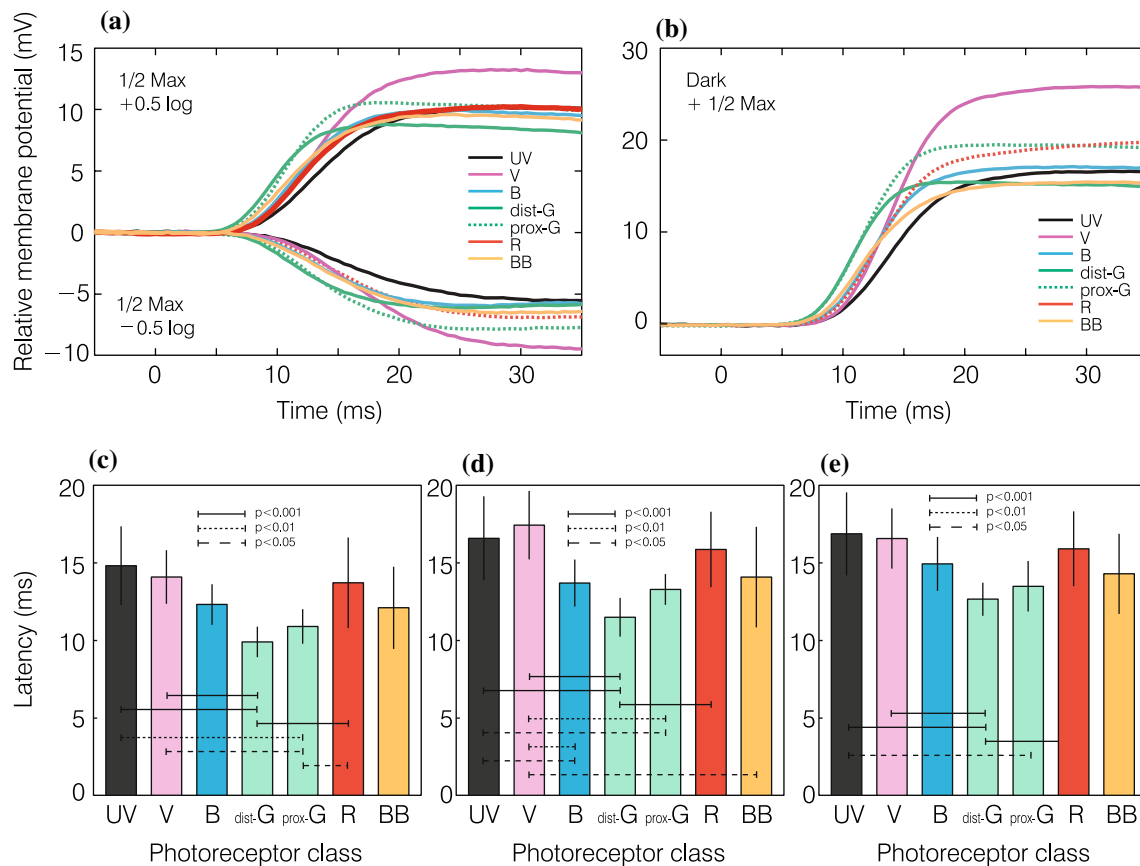


Fig. 3 Responses to the pulse stimulus. **a** Depolarizing (*top half*) and hyperpolarizing (*bottom half*) responses to incremental and decremental light pulses (± 0.5 log) with an initial intensity level that evoked a half maximum response in a given photoreceptor cell. Twenty 30 ms pulses were repeated and the average response was calculated. Each *line* shows a group average for each photoreceptor class. **b** Responses to light pulses from dark. Same format as in **a**.

c Latency to the time point where the membrane potential reaches 50 % of maximum depolarization in **a**. **d** Latency to the time point where the membrane potential reaches 50 % of the deepest hyperpolarization in **a**. **e** Latency to the time point where the membrane potential reaches 50 % of the maximum depolarization in **b**. Square pulse stimuli started at time zero and terminated at 30 ms in **a** and **b**

responses to incremental pulses were consistently shorter (~ 30 %) than hyperpolarizing responses to decremental pulses in all photoreceptor classes (Fig. 3a). The faster responses in dist-G and prox-G, and the differences in latency and in response magnitudes for incremental and decremental pulses were also consistently observed when steady background levels that evoked 1/4 and 3/4 maximum responses were used (data not shown).

Dark noise

Power density spectra of the dark noise demonstrate large variance in the low frequency range (Fig. 4a). However, by integration of the power density in the frequency range 0–20 Hz, the noise power was found to be clearly higher in the short-wavelength UV and V receptors (Fig. 4b). Sharp peaks at 50 Hz originated from the AC power supply that

necessarily stays visible in the spectra during recordings of the small-amplitude noise.

Discussion

The present study examined the photoreceptors of *Papilio xuthus* for their capability of encoding high frequency signals (10–100 Hz) in the temporal domain. The investigation of linear dynamic properties used white-noise modulated light input, instead of recently common “naturalistic” stimulation (Juusola and de Polavieja 2003; Frolov et al. 2012; Heimonen et al. 2012; Song et al. 2012). White noise stimulation is particularly amenable for pinpointing the response dynamics of the cells (Marmarelis and Marmarelis 1978), whereas the “naturalistic” stimulation is clearly superior when information transmission capabilities are of interest. When supplemented with steady-state and step-response

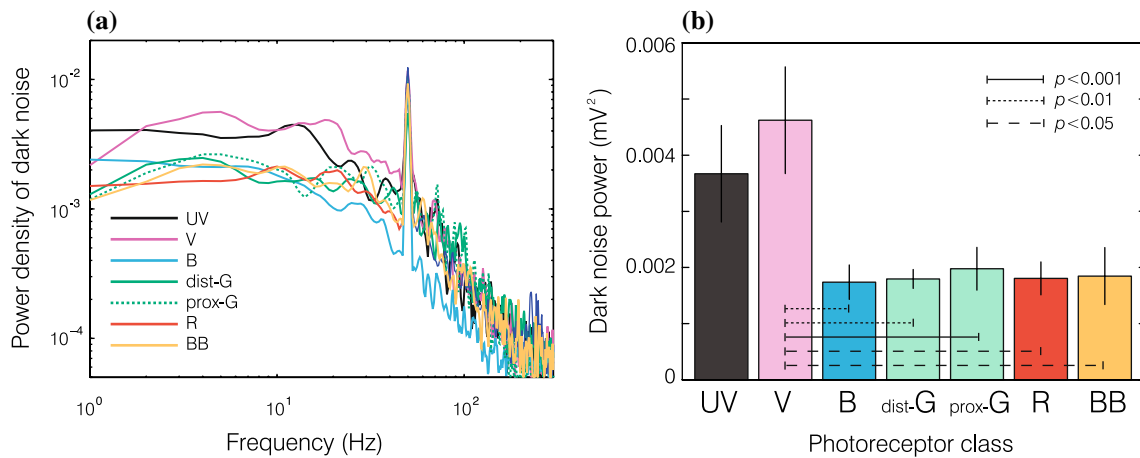


Fig. 4 Comparison of power density spectra of dark noise between photoreceptor types. **a** Mean spectra for different photoreceptor types in the low frequency range. **b** Integrated power density in the range of 1–20 Hz (one-way ANOVA followed by multiple comparisons)

analysis, we are confident that we have captured the essential properties of the different spectral classes of photoreceptors. Our main finding was that among the seven spectral classes of photoreceptors in *Papilio*, the dist-G class was here demonstrated to have the fastest dynamics as determined by high frequency gain functions in white-noise analyses and by response latencies to step changes of light intensity. The temporal response properties of the prox-G, B, BB and R receptors are intermediate. The UV and V classes were found to be slowest dynamically. The speed of all *Papilio xuthus* photoreceptors including the dist-G in the current study is comparable to that of the photoreceptors in *Bombus terrestris* (Vähäkainu et al. 2013) and that of the R1-6 photoreceptors of flies, which are much faster than their R7/8 photoreceptors for color and polarization vision (Juusola et al. 1994; Anderson and Laughlin 2000). The photoreceptor speed of *Papilio xuthus* overall is also faster than R7/8 photoreceptors of *Drosophila melanogaster* and the green-sensitive receptors of *Periplaneta americana* (Heimonen et al. 2012).

Photoreceptor cells of *Papilio* are classified into nine morphological types, R1–R9, according to the location of their rhabdomeres in the ommatidium and the morphology of their visual fibers (projection axons) and axon collaterals in the lamina (Takemura et al. 2005; Takemura and Arikawa 2006). The fastest spectral class, dist-G, in this study is found in exclusively the R3–4 morphological type that has no clear axon collaterals in the lamina where they terminate. All other spectral classes, including prox-G, belong to the R1–2 or R5–8 morphological types that have axon collaterals of various numbers and lengths in the lamina (the properties of R9 are not well characterized). The thick axon and the lack of clear collaterals in the dist-G class may contribute to shorter time constant of the passive membrane thus to faster dynamics. In flies, *Drosophila* and

Calliphora, R1-6 photoreceptors are dynamically faster than R7-8, and have a spectral peak at green and UV wavelengths (Anderson and Hardie 1996). Also in bumblebees, G receptors are the fastest (Skorupski and Chittka 2010). The temporal dynamics of photoreceptor responses depend on both passive and active (voltage-dependent) conductances in these insect groups (Skorupski and Chittka 2011; Vähäkainu et al. 2013). The response latency to incremental step signals is shorter than that to decremental stimuli (Fig. 3). This indicates that active conductances possibly enhance response dynamics also in *Papilio*. Photoreceptor cells of *Papilio* extend the visual fibers of various lengths into the lamina and medulla. The visual fibers attenuate high-frequency signal transfer to presynaptic endings, according to their cable properties (Hodgkin and Rushton 1946; Koch 1998) in flies (Van Hateren and Laughlin 1990). The variation of dynamics across different spectral types of photoreceptors in *Papilio*—when recorded in the retina—was found in this study to correlate only loosely with the length of the visual fibers that project to the lamina and the medulla (Takemura et al. 2005). A strong correlation was found in the fastest dist-G class that possesses a thick and short visual fiber terminating at 80 % depth of the lamina, and in the slowest UV and V classes, which have thin and long visual fibers terminating deep in the medulla. B, prox-G, R and BB classes, which were found to have intermediate dynamics, however, still possess short visual fibers that terminate at ~80 % depth in the lamina as in the fastest dist-G class.

UV and V receptors exhibited significantly larger dark noise than others (Fig. 4). Taken together with their relatively slow dynamics, the large dark noise implies large gain in terms of mV/photon. This probably has its origin in the electrical structure of the cells, i.e., in processes after the transduction mechanisms, analogously as in the R7/R8

photoreceptors in flies (Anderson and Laughlin 2000). This could be verified by recording single photon responses, but those are, unfortunately, too small to be observed in intracellular recording in *Papilio*.

The fast dynamics found in the dist-G receptors in *Papilio* may serve motion vision, which requires high temporal acuity. According to Land (1999), complete motion blur occurs when image velocity exceeds twice the acceptance angle per response time gate. The acceptance angle of a single ommatidium in *Papilio* ranges between 1.5° and 2.0° (Horridge et al. 1983). If we assume 20 ms for the time gate of dist-G receptors in *Papilio* (equivalent to the 3 dB frequency), Land's formula yields 175°/s for complete blur, and 87.5°/s for 50 % blur. Although no behavioral data are available for rotational speeds in flying *Papilio*, these values are reasonable estimates of upper limit. Fast flying insects tend to have faster photoreceptors as obvious adaptation for processing fast image motion (Laughlin and Weckström 1993; Weckström and Laughlin 1995; Skorupski and Chittka 2011).

The lack of axon collaterals in the dist-G receptors of *Papilio* suggests involvement of this class of photoreceptors in achromatic visual processes. While photoreceptors of other spectral classes contact each other across lamina cartridges through axon collaterals possibly contributing to the chromatic process (or color vision), dist-G receptors' thick and singular axons terminate onto the large monopolar cells within the lamina cartridge without ramification (Takemura et al. 2005). Green-sensitive photoreceptors of various insect species have been shown to drive achromatic motion-induced behaviors (Kaiser 1975; Heisenberg and Buchner 1977; Srinivasan and Lehrer 1984; Yamaguchi et al. 2008). Optomotor responses in butterflies are also achromatic and their action spectrum is close to the spectral sensitivity of the dist-G receptors in *Papilio* (Horridge et al. 1984). We have recorded from directional-selective motion-sensitive neurons in the optic lobe of *Papilio* and observed that they ceased responding to a moving chromatic grating when it loses luminosity contrast while the chromatic contrast remained (unpublished observations). The achromatic visual system is faster than the chromatic one also in mammals (Kaiser and Boynton 1995; He and MacLeod 1997). The prox-G receptors consistently showed slower dynamics than the dist-G receptors (Figs. 2, 3). The prox-G receptors (R5-8) have extensive axon collaterals across lamina cartridges, which implies interaction with other spectral classes for chromaticity processing. We hypothesize that dist-G and prox-G receptors are mainly involved in motion and color vision, respectively, despite similar spectral sensitivities. The difference in their dynamics is probably due to the differences in membrane conductances, rather than transduction mechanisms or morphology of passive membrane, as shown in other

insect species (Anderson and Hardie 1996; Anderson and Laughlin 2000; Skorupski and Chittka 2010; Vähäkainu et al. 2013).

This study showed that a lepidopteran insect, *Papilio xuthus*, invests metabolically costly high-frequency processes in the dist-G receptors as other insect groups do so for their motion vision (Laughlin et al. 1998).

Acknowledgments This work was supported by the SOKENDAI visiting professorship to MKa, the JSPS (Japanese Society for Promotion of Science) Grants-in-Aid for Scientific Research C to MKi (24570084) and A to KA (26251036), JSPS open partnership joint research project (Finland) to KA, the NARO (National Agriculture and Food Research Organization) grant for SIP (Strategic Innovation Promotion) Program "Technologies for creating next-generation agriculture, forestry and fisheries" to KA, and the research grant from the Academy of Finland (269332) to MW.

References

- Anderson J, Hardie RC (1996) Different photoreceptors within the same retina express unique combinations of potassium channels. *J Comp Physiol A* 178:513–522
- Anderson JC, Laughlin SB (2000) Photoreceptor performance and the co-ordination of achromatic and chromatic inputs in the fly visual system. *Vision Res* 40:13–31
- Arikawa K (2003) Spectral organization of the eye of a butterfly, *Papilio*. *J Comp Physiol A* 189:791–800
- Arikawa K, Inokuma K, Eguchi E (1987) Pentachromatic visual system in a butterfly. *Naturwissenschaften* 74:297–298
- Arikawa K, Mizuno S, Scholten DG, Kinoshita M, Seki T, Kitamoto J, Stavenga DG (1999) An ultraviolet absorbing pigment causes a narrow-band violet receptor and a single-peaked green receptor in the eye of the butterfly *Papilio*. *Vision Res* 39:1–8
- Arikawa K, Mizuno S, Kinoshita M, Stavenga DG (2003) Coexpression of two visual pigments in a photoreceptor causes an abnormally broad spectral sensitivity in the eye of a butterfly, *Papilio xuthus*. *J Neurosci* 23:4527–4532
- Bendat JS, Piersol AG (1971) Random data: analysis and measurement procedures. John Wiley and Sons Inc, New York
- Dyer AG, Arikawa K (2014) A hundred years of color studies in insects: with thanks to Karl von Frisch and the workers he inspired. *J Comp Physiol A* 200:409–410
- Friedrich M, Wood EJ, Wu M (2011) Developmental evolution of the insect retina: insights from standardized numbering of homologous photoreceptors. *J Exp Zool B* 316:484–499
- Frolov R, Immonen EV, Vähäsöyrinki M, Weckström M (2012) Postembryonic developmental changes in photoreceptors of the stick insect *Carausius morosus* enhance the shift to an adult nocturnal life-style. *J Neurosci* 32:16821–16831
- Hardie RC (1985) Functional organization of the fly retina. In: Ottosson D (ed) *Progress in Sensory Physiology*, vol 5. Springer, Berlin Heidelberg New York Toronto, pp 1–79
- He S, MacLeod DI (1997) Local nonlinearity in S-cones and their estimated light-collecting apertures. *Vision Res* 38:1001–1006
- Heimonen K, Immonen EV, Frolov RV, Salmela I, Juusola M, Vähäsöyrinki M, Weckström M (2012) Signal coding in cockroach photoreceptors is tuned to dim environments. *J Neurophysiol* 108:2641–2652
- Heisenberg M, Buchner E (1977) The role of retinula cell types in visual behavior of *Drosophila melanogaster*. *J Comp Physiol A* 117:127–162

- Hodgkin A, Rushton W (1946) The electrical constants of a crustacean nerve fibre. *Proc Roy Soc B* 133:444–479
- Horridge GA, Marčelja L, Jahnke R, Matič T (1983) Single electrode studies on the retina of the butterfly *Papilio*. *J Comp Physiol A* 150:271–294
- Horridge GA, Marčelja L, Jahnke R (1984) Color vision in butterflies 1. Single colour experiments. *J Comp Physiol A* 155:529–542
- Juusola M, de Polavieja GG (2003) The rate of information transfer of naturalistic stimulation by graded potentials. *J Gen Physiol* 122:191–206
- Juusola M, Kouvalainen E, Järvilehto M, Weckström M (1994) Contrast gain, signal-to-noise ratio, and linearity in light-adapted blowfly photoreceptors. *J Gen Physiol* 104:593–621
- Kaiser W (1975) The relationship between visual movement detection and colour vision in insects. In: Horridge GA (ed) *The compound eye and vision in insects*. Clarendon Press, Oxford, pp 359–377
- Kaiser PK, Boynton RM (ed) (1995) *Human colour vision*, 2nd edn. In: *Optical Society of America*, Washington DC, p 652
- Kinoshita M, Arikawa K (2014) Color and polarization vision in foraging *Papilio*. *J Comp Physiol A* 200:513–526
- Kinoshita M, Kurihara D, Tsutaya A, Arikawa K (2006) Blue and double-peaked green receptors depend on ommatidial type in the eye of the Japanese yellow swallowtail *Papilio xuthus*. *Zool Sci* 23:199–204
- Koch C (1998) *Biophysics of computation: information processing in single neurons*. Oxford University Press, Oxford, New York etc
- Koshitaka H, Kinoshita M, Vorobyev M, Arikawa K (2008) Tetrachromacy in a butterfly that has eight varieties of spectral receptors. *Proc Roy Soc B* 275:947–954
- Kv Frisch (1914) *Der Farbensinn und Formensinn der Biene*. *Zool Jb Physiol* 37:1–238
- Land MF (1999) Motion and vision: why animals move their eyes. *J Comp Physiol A* 185:341–352
- Laughlin S, Weckström M (1993) Fast and slow photoreceptors—a comparative study of the functional diversity of coding and conductances in the Diptera. *J Comp Physiol A* 172:593–609
- Laughlin SB, van Steveninck RRD, Anderson JC (1998) The metabolic cost of neural information. *Nat Neurosci* 1:36–41
- Lehrer M, Wehner R, Srinivasan M (1985) Visual scanning behavior in honeybees. *J Comp Physiol A* 157:405–415
- Lehrer M, Wehner R, Srinivasan M (1989) How honeybees measure their distance from objects of unknown size. *J Comp Physiol A* 165:605–613
- Livingstone M, Hubel D (1988) Segregation from color, movement, and depth—atomy, physiology, and perception. *Science* 240:740–749
- Marmarelis PZ, Marmarelis VZ (1978) *Analysis of physiological systems: the white-noise approach*. Plenum Press, New York
- Schnaitmann C, Garbers C, Wachtler T, Tanimoto H (2013) Color discrimination with broadband photoreceptors. *Curr Biol* 23:2375–2382
- Skorupski P, Chittka L (2010) Differences in photoreceptor processing speed for chromatic and achromatic vision in the bumblebee, *Bombus terrestris*. *J Neurosci* 30:3896–3903
- Skorupski P, Chittka L (2011) Photoreceptor processing speed and input resistance changes during light adaptation correlate with spectral class in the bumblebee, *Bombus impatiens*. *PLoS One* 6:e25989
- Song Z, Postma M, Billings SA, Coca D, Hardie RC, Juusola M (2012) Stochastic, adaptive sampling of information by microvilli in fly photoreceptors. *Curr Biol* 22:1371–1380
- Srinivasan MV, Lehrer M (1984) Temporal acuity of honeybee vision: behavioural studies using moving stimuli. *J Comp Physiol A* 155:297–312
- Strausfeld NJ, Lee J-K (1991) Neuronal basis for parallel visual processing in the fly. *Vis Neurosci* 7:13–33
- Takemura SY, Arikawa K (2006) Ommatidial type-specific interphotoreceptor connections in the lamina of the swallowtail butterfly, *Papilio xuthus*. *J Comp Neurol* 494:663–672
- Takemura S, Kinoshita M, Arikawa K (2005) Photoreceptor projection reveals heterogeneity of lamina cartridges in the visual system of the Japanese yellow swallowtail butterfly, *Papilio xuthus*. *J Comp Neurol* 483:341–350
- Vähäkainu A, Vähäsöyrinki M, Weckström M (2013) Membrane filtering properties of the bumblebee (*Bombus terrestris*) photoreceptors across three spectral classes. *J Comp Physiol A* 199:629–639
- Van Hateren J, Laughlin S (1990) Membrane parameters, signal transmission, and the design of a graded potential neuron. *J Comp Physiol A* 166:437–448
- Wakakuwa M, Kurasawa M, Giurfa M, Arikawa K (2005) Spectral heterogeneity of honeybee ommatidia. *Naturwissenschaften* 92:464–467
- Wakakuwa M, Stavenga DG, Arikawa K (2007) Spectral organization of ommatidia in flower-visiting insects. *Photochem Photobiol* 83:27–34
- Wardill TJ, List O, Li X, Dongre S, McCulloch M, Ting CY, O’Kane CJ, Tang S, Lee CH, Hardie RC, Juusola M (2012) Multiple spectral inputs improve motion discrimination in the *Drosophila* visual system. *Science* 336:925–931
- Weckström M, Laughlin SB (1995) Visual ecology and voltage-gated ion channels in insect photoreceptors. *Trends Neurosci* 18:17–21
- Yamaguchi S, Wolf R, Desplan C, Heisenberg M (2008) Motion vision is independent of color in *Drosophila*. *Proc Natl Acad Sci USA* 105:4910–4915